J Solid State Electrochem (2002) 6: 311–319
DOI 10.1007/s100080100239

ORIGINAL PAPER

Ģ. Vītiņš · G. Ķizāne · A. Lūsis · J. Tīliks

Electrical conductivity studies in the system Li_2TiO_3-$Li_{1.33}Ti_{1.67}O_4$

Received: 26 September 2000 / Accepted: 10 July 2001 / Published online: 16 October 2001

Abstract Electrical conductivity in the monoclinic Li_2TiO_3, cubic $Li_{1.33}Ti_{1.67}O_4$, and in their mixture has been studied by impedance spectroscopy in the temperature range 20–730 °C. Li_2TiO_3 shows low lithium ion conductivity, $\sigma_{300}\approx10^{-6}$ S/cm at 300 °C, whereas $Li_{1.33}Ti_{1.67}O_4$ has 3×10^{-8} at 20 °C and 3×10^{-4} S/cm at 300 °C. Structural properties are used to discuss the observed conductivity features. The conductivity dependences on temperature in the coordinates of $1000/T$ versus $\log_e(\sigma T)$ are not linear, as the conductivity mechanism changes. Extrinsic and intrinsic conductivity regions are observed. The change in the conductivity mechanism in Li_2TiO_3 at around 500–600 °C is observed and considered as an effect of the first-order phase transition, not reported before. Formation of solid solutions of $Li_{2-x}Ti_{1+x}O_3$ above 900 °C significantly increases the conductivity. Irradiation by high-energy (5 MeV) electrons causes defects and the conductivity in Li_2TiO_3 increases exponentially. A dose of 144 MGy yields an increase in conductivity of about 100 times at room temperature.

Keywords Lithium metatitanate · Lithium titanate · Ion conductivity · Solid solutions

Introduction

Lithium metatitanate, β-Li_2TiO_3 (the monoclinic form), has been found as a promising material for the blanket zone, where the $^6Li(n,\alpha)^3H$ reaction takes place in a D-T fusion reactor [1]. Particularly, β-Li_2TiO_3 shows a faster tritium release than Li_4SiO_4, which has been studied for these reasons. It has also a good chemical and radiation stability [1]. In these aspects, Li_2TiO_3 becomes superior over other lithium-containing oxide compounds such as Li_2O, Li_6ZrO_8, Li_2ZrO_3, Li_4ZrO_4, Li_2SiO_3, Li_4SiO_4, Li_8PbO_6, or γ-$LiAlO_2$, tested for tritium breeding previously [2, 3, 4]. It has been recognized earlier that lithium ion conductivity is related to the diffusion of tritium ions in these materials: the higher is the lithium ion conductivity, the higher is the tritium diffusion [2, 3, 4]. Particularly, Noda et al. [2] have observed that the order of magnitude of lithium ion conductivity in Li_2O, γ-$LiAlO_2$, and Li_8ZrO_6 is the same as that of tritium diffusion in these compounds. The relation of the magnitudes can be written as: $\sigma(Li_8ZrO_6) > \sigma(Li_2O) > \sigma(\gamma\text{-}LiAlO_2)$, corresponding to $D(Li_8ZrO_6) > D(Li_2O) > D(\gamma\text{-}LiAlO_2)$. Thus, lithium ion conductivity values may be useful for evaluating tritium diffusion in solid tritium breeder materials. Conductivity data for the system Li_2TiO_3-$Li_{1.33}Ti_{1.67}O_4$ (with the Li_2O:TiO_2 ratio in range from 50:50 to 28.6:71.4) are insufficient thus far. This pseudo-binary system corresponds to the situation which appears during the lithium burn-up in the reaction $^6Li(n,\alpha)^3H$ at 500–900 °C.

Electrophysical properties of blanket ceramics are of importance concerning the appearance of electric and magnetic fields in fusion reactors during plasma operations. If the blanket zone forms a closed circuit, electric and changing magnetic fields may cause an electric current in the blanket material, leading to changes in its composition and properties. Particularly, studies of the electrophysical properties and electric degradation of Li_4SiO_4 from this viewpoint have been reported by Tamuzhs et al. [5].

Since the 1970s, H^+, Li^+, Na^+, and Ag^+ ion conducting materials have been of great interest for their application in electrochemical devices, e.g. sensors, batteries, and electrochromic devices. Several ion conducting compounds having high ion conductivity have been found to be useful as solid electrolytes or electrode

Ģ. Vītiņš (✉) · G. Ķizāne · J. Tīliks
Laboratory of Radiation Chemistry of Solids,
Department of Chemistry, University of Latvia,
4 Kronvalda Boulevard, 1010 Riga, Latvia
E-mail: vitinsg@latnet.lv
Tel.: +37-1-7187817
Fax: +37-1-7112583

Ģ. Vītiņš · A. Lūsis
Institute of Solid State Physics, University of Latvia,
8 Ķengaraga Street, 1063 Riga, Latvia

materials. Still, a search for new ion conductors is at a premium in order to extend the choice of the materials and to add to facts in order to better understand the ion conductivity phenomena in solids. The highest Na^+ conductivity is found in Na-β-alumina ($\sigma_{25}=10^{-3}$–10^{-2} S/cm with activation energy $E_a=0.14$–0.34 eV [6, 7, 8]) and $Na_3Zr_2Si_2PO_{12}$ (NASICON, $\sigma_{25}=6\times10^{-4}$ S/cm, $E_a=0.39$ eV [9, 10, 11]). The highest Ag^+ conductivity is found in AgI [12, 13, 14] and Ag_4RbI_5 ($\sigma_{25}=0.25$ S/cm, $E_a=0.10$ eV [14, 15]). Solid lithium compounds tend to have lower conductivity since the lithium ions, having a smaller ion radius, are bound stronger. Well-known lithium ion conductors are $Li_3Sc_2(PO_4)_3$ ($\sigma_{300}=0.02$ S/cm, $E_a=0.93$ eV at 90–171 °C and 0.28 eV at 282–467 °C [16]), Li_3N ($\sigma_{25}=10^{-3}$ S/cm, $E_a=0.20$ eV [17, 18]), which, however, is a thermally and moisture unstable material, and $La_{0.51}Li_{0.34}TiO_{2.94}$ ($\sigma_{25}=10^{-3}$ S/cm [19, 20]). Lithium ion conductivity parameters in other oxide compounds, including Li_4SiO_4, Li_4ZrO_4, Li_8ZrO_6, etc., have been summarized by Ohno et al. [21] and indicate lower ion transport properties. Sufficiently wide bottlenecks in ion transport channels, the presence of free interstices (vacancies) energetically advantageous for ion delocalization, and polarizability of the conducting ions or a rigid network allow fast ion mobility in these compounds and structures.

Other types of lithium ion conductors are known. These are transition metal oxide compounds, often having higher electron conductivity than lithium ion conductivity and, thus, they often are named as mixed conductors. These compounds often form a wide range of solid solutions with lithium. This property is useful in cathode materials for lithium rechargeable batteries, as the structure alters slightly. In mixed conductors, lithium ion conductivity is promoted by high electron mobility in the transition metal oxide array. Several insertion compounds have become popular with their superior cathode material performance, for instance, the spinel-type $Li_xMn_2O_4$ ($x=0$–2; $D_{Li}=10^{-8}$–10^{-9} cm^2/s [22, 23]; electron conductivity $\sigma_e=10^{-4}$–10^{-3} S/cm [24]). Here we should note that $Li_{1.33}Ti_{1.67}O_4$ (or $Li_4Ti_5O_{12}$), which is studied in the present paper, takes a spinel-type structure as well and, thus, we can expect some similar tendencies to $LiMn_2O_4$ in its ion transport properties. Yet $Li_{1.33}Ti_{1.67}O_4$ has already been tested as an insertion electrode material and has shown a highly reversible lithium insertion at 1.5 V versus Li in the solid solution range $x=0$–1 in $Li_xLi_{1.33}Ti_{1.67}O_4$ at 120 °C with a current density of 50 μA/cm^2 [25].

Previous studies of the phase diagram of the pseudobinary system along the join Li_2O-TiO_2 have shown the existence of several ternary compounds [26, 27]: Li_4TiO_4 (33.3 mol% TiO_2; isostructural [28, 29] with Li_4GeO_4), Li_2TiO_3 (50 mol% TiO_2; having a monoclinic (β) NaCl-type to cubic (γ) NaCl-type phase transition at 1150 °C [1, 26, 27]; isostructural [30, 31] with Li_2SnO_3 and Li_2MnO_3), $Li_2Ti_2O_5$ (66.7 mol% TiO_2; spinel type with $a=8.30$ Å [32]), $Li_4Ti_5O_{12}$ (71.4 mol% TiO_2; spinel type with $a=8.36$ Å [25, 27]), and R-$Li_2Ti_3O_7$ (75 mol% TiO_2; ramsdelite type, stable at above 940 °C). Particularly, R-$Li_2Ti_3O_7$ can be obtained in a metastable state by rapid cooling. On repeated gradual heating the compound preserves the ramsdelite structure until 500 °C, where it transforms to a new metastable hexagonal phase H-$Li_2Ti_3O_7$, which decomposes into TiO_2 and $Li_4Ti_5O_{12}$ above 800 °C [27]. Mikkelsen [27] reports another important feature for compositions of 50–65 mol% TiO_2. They have observed heat effects around 930 °C, which are explained by existence of monoclinic phase solid solutions of $Li_{2-4x}Ti_xTiO_3$ above 930 °C. However, the authors [27] report a dependence of X-ray diffraction patterns on the cooling rate and, thus, miscibility borders of composition and of temperature are still uncertain for the composition range 50–65 mol% TiO_2. In the present study we use this fact in order to explain remarkable variations in the conductivity of several specimens prepared under different conditions. Besides, this observation means that the system in the range 50–65 mol% TiO_2 can only be defined clearly by using both X-ray diffraction and elemental composition data. Solid solutions of the lithium-rich monoclinic phase of $Li_2Ti_{1-x}Li_{x/4}O_3$ or the lithium-rich spinel phase of $Li_4Ti_{5-x/4}Li_xO_{12}$ have not been reported thus far. The formation of such solutions is highly hindered by structural limits, as one Ti^{4+} must be substituted by four Li^+ to compensate the negative charge of the array of oxygen atoms.

Few studies of the conductivity in lithium titanates have been done before. Among these, metastable R-$Li_2Ti_3O_7$ has shown the highest conductivity of 10^{-4} S/cm at room temperature, as reported by Roth et al. [33], and it has a significant conductivity anisotropy ($\sigma_c/\sigma_b=7$; $\sigma_b/\sigma_a=4$ [34]) caused by its one-dimensional channel structure. Electron conductivity is found to be less than 1% of the lithium ion conductivity in this compound. The conductivity of solid solutions of heterovalent substitution in $Li_{2-3x}Al_xTiO_3$ ($x=0$, 0.05, 0.3) and $Li_{2-4x}Ti_xTiO_3$ has been measured in the temperature range 400–800 °C [35]. Li^+ ions are considered as the only charge carriers. By extrapolation, at 300 °C the conductivity can be estimated to be of the order 10^{-6}–10^{-5} S/cm for these materials. The conductivity increases in substituted compounds. No activation energies or preexponential factors are given for the conductivity temperature dependences [35].

In the present study we consider the conductivity obtained for Li_2TiO_3 (50 mol% TiO_2), $Li_{1.33}Ti_{1.67}O_4$ (71.4 mol% TiO_2), and for intermediate compositions, 86.7 mol% Li_2TiO_3 × 13.3 mol% TiO_2 (56.7 mol% TiO_2; or for a solid solution of Ti^{4+} substitution for Li^+: $Li_{1.815}Ti_{0.0463}TiO_3$), and 74.7 mol% Li_2TiO_3 × 25.6 mol% TiO_2 (62.8 mol% TiO_2; or for solid solution: $Li_{1.627}Ti_{0.094}TiO_3$). These titanium-rich compositions would correspond to lithium burn-up in the blanket zone. Conductivity data would indicate whether the tritium diffusion will increase or not in these materials. The influence of high-energy irradiation (accelerated

electrons of 5 MeV) on the conductivity of Li_2TiO_3 is also tested and presented.

Experimental

Synthesis

Several specimens were prepared for the conductivity studies. Li_2TiO_3, obtained from the Factory of Rare Element Materials of Novosibirsk (Russia), was pressed into pellets (diameter = 1 cm, $p = 1$ GPa) and sintered at 960 °C for 6 h in closed furnace, then slowly cooled from furnace to room temperature in one day. Other Li_2TiO_3 specimens were prepared by the ordinary solid state reaction technique, mixing pure Li_2CO_3 (mp 725 °C [36]) and TiO_2 in amounts close to the right stoichiometry. Then they were heated at 750–770 °C for 24 h. Afterwards the powders were reground and pressed into pellets (diameter = 1 cm, $p = 640$ MPa) and sintered at 890–900 °C for 24–30 h. Studies on the preparation of Li_2TiO_3 have been reported previously [36, 37]. Particularly, the heat effect of the reaction between Li_2CO_3 and TiO_2 to form Li_2TiO_3 has a maximum at 800 °C [36]. However, higher temperatures are desired in order to obtain the material in a well-crystallized state. Other specimens were prepared in a similar manner. Their preparation conditions are described in Table 1.

X-ray powder diffraction and scattered reflectance spectroscopy

The prepared materials were controlled by X-ray powder diffraction using Ni-filtered Co K_α radiation ($\lambda_{\alpha 1} = 1.78897$, $\lambda_{\alpha 2} = 1.79285$ Å) and a scan rate of 0.05° 2θ/4 s. For some samples, Rietveld refinement by the computing program SR5 [38, 39, 40, 41, 42] was carried out in order to confirm the phase and to calculate the unit cell parameters. The materials were also controlled by scattered reflectance spectroscopy [43] using a spectrophotometer "Specord M-40" in a wavelength range from 240 through 900 nm with an incident beam angle of 9°, and with a distance of 10 cm from the sample to the detector. Spectra were recorded versus MgO as a white material.

Impedance measurements

In order to determine the conductivity of the materials, impedance measurements were performed in the frequency range from 100 Hz to 20 MHz on a Hewlett Packard 4194A impedance/gain-phase analyser, which works as an autobalancing a.c. bridge [44]. The parasitic inductance of the leads was compensated. The parallel capacitance of the wires was determined and also subtracted. The amplitude of the a.c. signal was set in the range 10–500 mV, depending on the resistance of the material. The impedance was measured in the range 20–730 °C in air, both increasing and decreasing the temperature. Ceramic pellets, covered by Ag (obtained from decomposition of Ag_2CO_3 paste at 800–820 °C) on their opposite sides, were used for the two-probe measurements.

Irradiation

The irradiation of Li_2TiO_3 by different doses was performed by a linear electron accelerator EUL-5 with $E_{e^-} = 5$ MeV and $I = 4.5$ μA/cm^2, corresponding to a mass absorption coefficient of 2.55 g/cm^2, a linear track length of 0.97 cm, and $P = 32$ MGy/h in Li_2TiO_3. During the irradiation the Li_2TiO_3 pellets, with a total thickness less than 0.4 cm, were cooled in a special sample holder to keep them at a temperature around 50–70 °C. Prior to the irradiation the samples were covered by Ag (10–15 μm) electrodes.

Results and discussion

Structure and X-ray phase analysis

X-ray powder diffraction confirmed monoclinic Li_2TiO_3 as a single phase in the specimens LT4, LT8, LT10, and LT14 (see Table 1). Addition of extra lithium in form of Li_2CO_3 promotes the formation of larger crystals and denser sintering, yielding a pellet density 87–91% of the theoretical density (TD) of 3.42 g/cm^3. Unit cell

Table 1 Preparation, density (in % of theoretical density, TD), dielectric constant (ϵ) at 5–10 MHz, and conductivity (at 300 °C) for the lithium titanium oxide materials studied. The Li_2TiO_3 powder from Novosibirsk has lithium deficiency originally

Material	Code	Preparation	Density (%TD)	ϵ	$\sigma_{300}\times10^6$ (S/cm)
Li_2TiO_3	LT4	(1) 24 h, 770 °C (2) 17 h, 850 °C (3) +3.6 mol% Li^+, 15 h, 853 °C (4) 22 h, 850 °C	75	11.8	0.06
Li_2TiO_3	LT8	(1) 20 h, 750 °C (2) 12 h, 860 °C	78	16	1
Li_2TiO_3	LT10	1) +1.5 mol% Li^+, 20 h, 770 °C 2) 30 h, 900 °C.	91	20.7	2
Li_2TiO_3	LT14	(1) +1.5 mol% Li^+, 20 h, 760 °C (2) 15 h, 850 °C	87	23	4
Li_2TiO_3 + 30.8 mol% $Li_{1.33}Ti_{1.67}O_4$ (+25.6 mol% TiO_2)	LT12	(1) 20 h, 770 °C (2) 24 h, 900 °C	75	13.9	4
$Li_{2-4x}Ti_{1+x}O_3 + yLi_{1.33}Ti_{1.67}O_4$, where y = 2–4 mol%	LT1	A powder from Novosibirsk sintered at 960 °C for 6 h	77	13.5	0.5
$(Li_{2-4x}Ti_{1+x}O_3 + yLi_{1.33}Ti_{1.67}O_4)$ + 16.4 mol% $Li_{1.33}Ti_{1.67}O_4$	LT2	A powder from Novosibirsk +13.3 mol% TiO_2 sintered at 960 °C for 6 h	75	13.6	3.5
$(Li_{2-4x}Ti_{1+x}O_3 + yLi_{1.33}Ti_{1.67}O_4)$ + 30.8 mol% $Li_{1.33}Ti_{1.67}O_4$	LT3	A powder from Novosibirsk +25.6 mol% TiO_2 sintered at 960 °C for 6 h	74	14.1	25
$Li_{1.33}Ti_{1.67}O_4$	LT13	(1) 7 h, 770 °C (2) 28 h, 890–900 °C	75	17.5	280

parameters of $a = 5.067(2)$, $b = 8.779(3)$, $c = 9.748(2)$ Å, and $\beta = 100.08(5)°$ obtained for LT4 are close to the values for Li_2TiO_3 reported previously [27, 30, 45]. In LT4 the Rietveld calculation confirmed a strong preferred orientation with a March factor 0.73 in vector (0,0,1). The plate-type crystallites were textured during the pressing of the pellets in this preparation (LT4). Preparations of the final pellets using the powder reacted below 800 °C yielded no preferred orientation as the powder is of low crystallinity. X-ray diffraction confirmed a single cubic ($a = 8.357$ Å) phase of spinel-related $Li_{1.33}Ti_{1.67}O_4$ in the specimen LT13. The other specimens (LT1, LT2, LT3, and LT12) are two-phase (monoclinic/cubic) materials having the diffraction line intensity ratio $I_{cub}(400)/I_{mon}(-133)$ equal to 0.05, 0.50, 0.75, and 0.75, respectively. The powder from Novosibirsk had some lithium shortage as the monoclinic phase was accompanied with significant traces of the cubic spinel-related phase [$I_{cub}(400) = 0.05\ I_{mon}(-133)$]. This intensity ratio corresponds to 2–4 mol% of $Li_{1.33}Ti_{1.67}O_4$. However, the phase composition cannot be determined exactly and it slightly varies depending on the sintering temperature and the cooling rate, as solid solutions of $Li_{2-4x}Ti_{1+x}O_3$ form around 930 °C [27]. Still, this border is uncertain and solid solutions may remain in a metastable state at an insufficiently slow cooling.

Scattered reflectance spectroscopy

Scattered reflectance spectra of Li_2TiO_3 (LT14, LT10) and $Li_{1.33}Ti_{1.67}O_4$ are shown in Fig. 1. Several features are to be noted for these materials. The materials are white, as remarkable light absorption starts at $\lambda < 350$ nm. Extrinsic electron energy levels in $Li_{1.33}Ti_{1.67}O_4$ provide light absorption at 364 nm (3.41 eV) of low intensity and strong absorption at 300 nm (4.13 eV). For Li_2TiO_3 the light absorption is shifted to a shorter wavelength, where the characteristic intensive band at 300 nm (4.54 eV) is seen, which also corresponds to an extrinsic energy absorption level, followed by the fundamental energy absorption at higher light energies. These optical spectra confirm that a wide gap separates the valence band from the conductivity band in these lithium titanates and no significant electron conductivity is expected in these materials. There are other features observed in the optical properties of Li_2TiO_3. Particularly, a slight absorption band at 534 nm (2.32 eV) and the twice as intense band at 416 nm (2.98 eV) were observed for Li_2TiO_3 samples which were prepared with a slight excess of lithium (e.g., 1.5–3.6 mol% Li^+) and heated at lower temperatures (e.g., at 770–850 °C) for a shorter time, for instance, 15 h in the cases of LT14 and LT4. These specimens had a slight brownish tinge. The energy absorption bands reduce when longer heat treatments at higher temperatures are applied, as is seen in Fig. 1 for LT10. The present observations allow us to propose that a very slight substitution of lithium for titanium occurs in Li_2TiO_3 and the solid solution of $Li_2Ti_{1-x}Li_{x/4}O_3$ forms. The electronic structure of lithium metatitanate is now affected by new local electron levels, corresponding to the bands at 416 and 534 nm. The scattering reflectance spectroscopy was also found to be an effective method to control traces of unreacted TiO_2, which were often observed for powders obtained from stoichiometric compositions in the preliminary heat treatments at 750–770 °C and having an absorption band at 390 nm characteristic for TiO_2 (rutile).

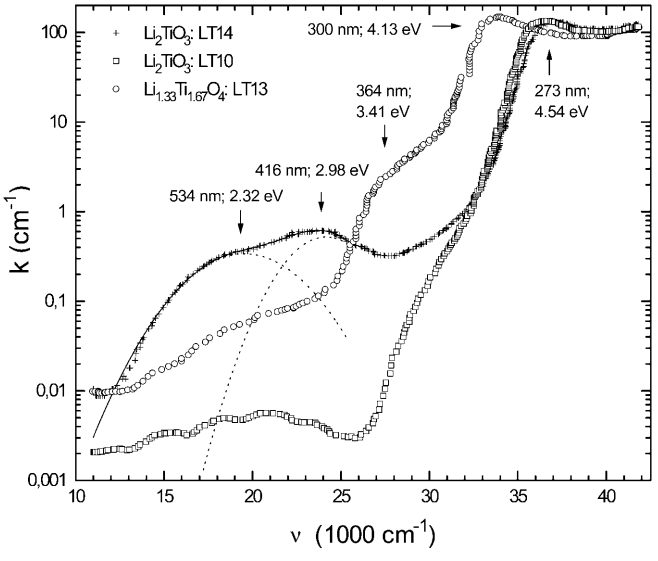

Fig. 1 Scattered reflectance spectra for Li_2TiO_3 (LT14, prepared with an extra 1.5 mol% Li^+ and sintered at 850 °C for 15 h), Li_2TiO_3 (LT10, stoichiometric, sintered at 900 °C for 30 h), and $Li_{1.33}Ti_{1.67}O_4$ (LT13, stoichiometric, sintered at 890–900 °C for 28 h)

Conductivity studies

Conductivity and dielectric constants were obtained from impedance data, which typically form a semicircle of regular shape with the centre more or less shifted below the real axis of the complex plane, as is often observed for solid ion conductors. At low frequencies the impedance of the electrode polarization was observed. The obtained impedance spectra correspond to bulk properties of the material as capacities observed are of the order $(1–10)\times10^{-12}$ F/cm, which is usual for oxide ceramics. Dielectric constants are presented in Table 1 and take values of 11.8–23, which are due to the relaxation of the rigid titanium-oxygen lattice and the electronic structure of lithium titanates.

The temperature dependences of the conductivity for the materials studied are depicted in Fig. 2 and Fig. 3. It is clear that the conductivity of Li_2TiO_3 is low and typically is in the range $(1–4)\times10^{-6}$ S/cm at 300 °C, also given in Table 1. Remarkably higher conductivity is apparent for $Li_{1.33}Ti_{1.67}O_4$. The conductivity is due to the lithium ion transport in these materials, as confirmed before, particularly for Li_2TiO_3 [35]. The electronic conductivity is expected to be insignificant, as can be

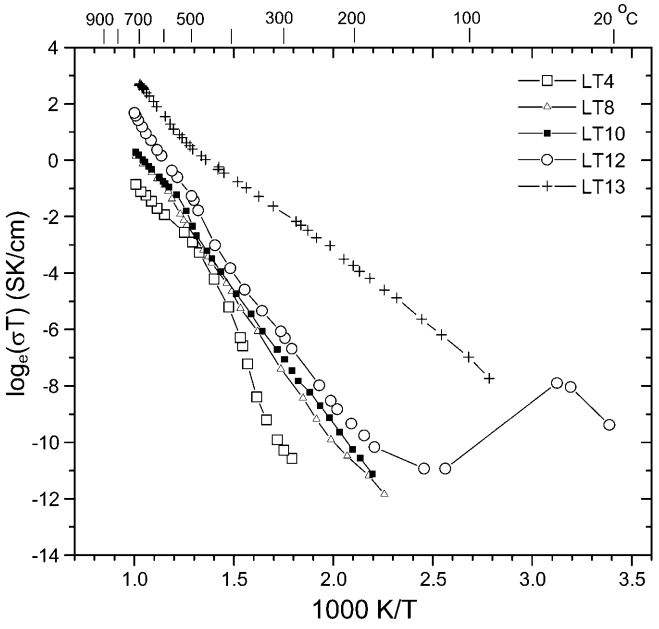

Fig. 2 Conductivity dependence on temperature for Li_2TiO_3 (LT4, LT8, LT10), $Li_2TiO_3 + 30.8$ mol% $Li_{1.33}Ti_{1.67}O_4$ (LT12), and $Li_{1.33}Ti_{1.67}O_4$

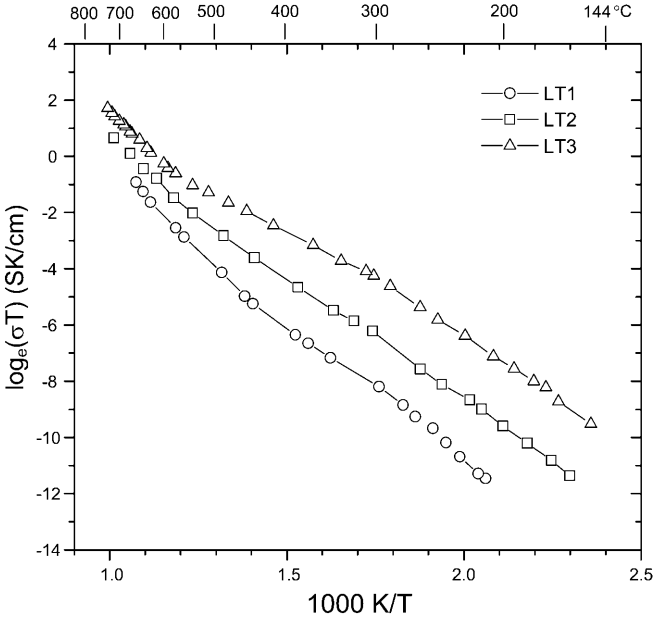

Fig. 3 Conductivity dependence on temperature for $Li_{2-4x}Ti_{1+x}O_3 + zLi_{1.33}Ti_{1.67}O_4$ specimens: LT1, LT2, and LT3 (see also Table 1)

concluded from the optical properties of lithium titanates and the electrode polarization. Neither could oxygen ion mobility be significant in these materials, since cubic close packing is essentially not a prospect for O^{2-} ion mobility. From the graphs it is seen that the conductivity dependences of temperature for the materials studied cannot be described by a single straight line which obeys the equation:

$$\sigma T = \sigma_0 \exp(-E_a/kT) \tag{1}$$

or in more elaborate form [46]:

$$\sigma = \frac{\gamma N e^2 c(1-c) z^2 a^2 v}{kT} \exp\left(\frac{\Delta S}{k}\right) \exp\left(-\frac{E_a}{kT}\right) \tag{2}$$

where γ is the correlation factor for the jumps, N is the total number of available sites per volume unit, e is the elementary charge, c is the fraction of mobile ions at these sites, z is the valence of charge carriers, a is the distance between the nearest sites, v is the ion vibration frequency close to 10^{13} Hz, ΔS is the change of entropy, k is the Boltzmann constant, and E_a is the activation energy. Instead, at least two or three straight lines have to be used in order to fit the plots in the temperature regions studied. The fit results are presented in Table 2. Similarities and differences in data are seen and can serve for several implications, considering the material structure and morphology as well.

In Fig. 2 the dependences of conductivity on temperature for two specimens of Li_2TiO_3 from different preparations (LT8 and LT10) are very similar, proving that the obtained data are characteristic for this material and structure. However, the curve for LT4 proceeds in a different way, taking values lower than those for LT8 and LT10. This particular feature can be explained by the strong preferred orientation in the direction (0,0,1) of Li_2TiO_3 crystallites in the measured pellet. The structure of Li_2TiO_3, shown in Fig. 4, clearly has a two-dimensional character in the cation arrangement. Lithium ion conductivity can occur in parallel to the *ab* plane; however, it is limited in the *c* direction by oxygen and titanium ion layers. Thus, conductivity will be limited, if lithium metatitanate crystals take an orientation with the *ab* plane being parallel to the electrode surfaces. At 300 °C the conductivity for LT4 is 6×10^{-8} S/cm, which is much lower than in LT8 and LT10 [conductivity of $(1–2)\times10^{-6}$ S/cm]. The particularly reduced dielectric constant of 11.8 for LT4 can be related to the anisotropy of the dielectric properties, which is caused by the same two-dimensional character of the Li_2TiO_3 structure.

Lithium ion conductivity in Li_2TiO_3 is hindered as all the normal lithium positions of octahedral coordination are occupied. Conductivity occurs by structure defects caused by lithium ions moving to tetrahedral interstices adjacent to the octahedral position. The mechanism can be modified by the fact that lithium ions take three types of octahedral positions, where lithium ions are bound by different energy. At 500–600 °C the activation energy of the conductivity consistently changes from 0.81–0.93 eV at lower temperatures to 0.59–0.61 eV at higher temperatures. There is a feature of a discontinuous transition at 500–600 °C in the plots of Fig. 2. Both lines, which fit curves of LT10 and LT8 at high and low temperatures, do not cross in the same points where the transition in the conductivity mechanism occurs. Thus, it can be concluded that a first-order phase change occurs in Li_2TiO_3 at 500–600 °C and causes the change in

Table 2 Activation energy and preexponential factor for conductivity of materials in the system Li_2TiO_3-$Li_{1.33}Ti_{1.67}O_4$. Parameters for $\log_e(\sigma T) = \log_e\sigma_0 - E_a/kT$ are given

Material	Code	$\log_e\sigma_0$ (S/cm)	E_a (eV)	T range (°C)
Li_2TiO_3	LT4	6.0(2)	0.59(2)	720–520
		14.0(3)	1.12(3)	526–405
		Transition	Transition	405–328
		8.7(1.5)	0.93(9)	328–285
	LT8	7.3(2)	0.61(2)	720–600
		11.1(1)	0.91(1)	600–170
	LT10	7.3(1)	0.60(2)	720–554
		Transition	Transition	520–424
		9.4(1)	0.81(1)	424–187
$Li_{1.33}Ti_{1.67}O_4$	LT13	12.3(1)	0.80(1)	702–562
		6.6(1)	0.42(1)	463–231
		8.0(1)	0.48(1)	231–86
Li_2TiO_3 + 30.8 mol% $Li_{1.33}Ti_{1.67}O_4$	LT12	14.2(3)	1.08(2)	726–672
		11.0(1)	0.82(1)	624–496
		10.0(2)	0.80(1)	222–438
$Li_{2-4x}Ti_{1+x}O_3 + yLi_{1.33}Ti_{1.67}O_4$, where y = 2–4 mol%	LT1	13.1(6)	1.14(4)	700–500
		5.5(2)	0.67(1)	400–300
		12.0(5)	0.98(3)	275–200
$(Li_{2-4x}Ti_{1+x}O_3 + yLi_{1.33}Ti_{1.67}O_4)$ + 16.4 mol% $Li_{1.33}Ti_{1.67}O_4$	LT2	13.3(5)	1.08(3)	720–537
		8.2(3)	0.72(2)	537–301
		9.6(3)	0.78(1)	301–162
$(Li_{2-4x}Ti_{1+x}O_3 + yLi_{1.33}Ti_{1.67}O_4)$ + 30.8 mol% $Li_{1.33}Ti_{1.67}O_4$	LT3	14.0(1)	1.07(1)	720–540
		6.9(1)	0.55(1)	540–300
		10.6(3)	0.73(1)	300–150

the conductivity mechanism. However, no previous DTA studies of Li_2TiO_3 [1, 27, 31] report heat effects in this temperature interval. It is likely that the transition is just displaced with only a slight increase in the entropy ΔS and has very little change on the thermal capacity of the material. Careful structural studies above this temperature are needed to confirm this phase transition. Particularly, Roux [1] reports changes in the X-ray diffraction pattern. However, no clear explanation is given on this effect. We assume that some kind of disordering possibly takes place at the transition temperature on heating. It releases ion (defect) transport and the activation energy decreases from 0.80–0.93 eV to 0.59–0.61 eV.

In Fig. 2 it is seen that the spinel-related $Li_{1.33}Ti_{1.67}O_4$ (LT13) has a much higher conductivity than does Li_2TiO_3. At 300 °C the conductivity in the spinel phase is about 100 times higher than that in lithium metatitanate, whereas at 20 °C the difference in the conductivities is larger and is estimated to be five orders of magnitude. At 20 °C, $Li_{1.33}Ti_{1.67}O_4$ has a conductivity of 3×10^{-8} S/cm, which is a relatively high value and can be considered as lithium ion conductivity. The electron conductivity should be insignificant in this case as electrode polarization was observed in impedance spectra and the material is colourless (see above). The temperature dependence of the conductivity in the Arrhenius plane for $Li_{1.33}Ti_{1.67}O_4$ is not simple again and can be approximated by three straight lines with the parameters given in Table 2. Below 463 °C the activation energy is 0.42–0.48 eV whereas above 562 °C it is 0.80 eV. Two mechanisms for lithium ion transport cause such a shape of the curves in Fig. 2. At low temperatures, defects possibly introduced by the grain surface determine the conductivity, whereas above 562 °C all the lithium ions in the structure contribute to the conductivity. The temperature dependence of the conductivity for similar shapes has been considered for Li_4ZrO_4 and Li_8ZrO_6 [21], and analogously the region having the lower slope at lower temperatures is explained by the extrinsic conductivity, and the high temperature region is ascribed to the intrinsic conduc-

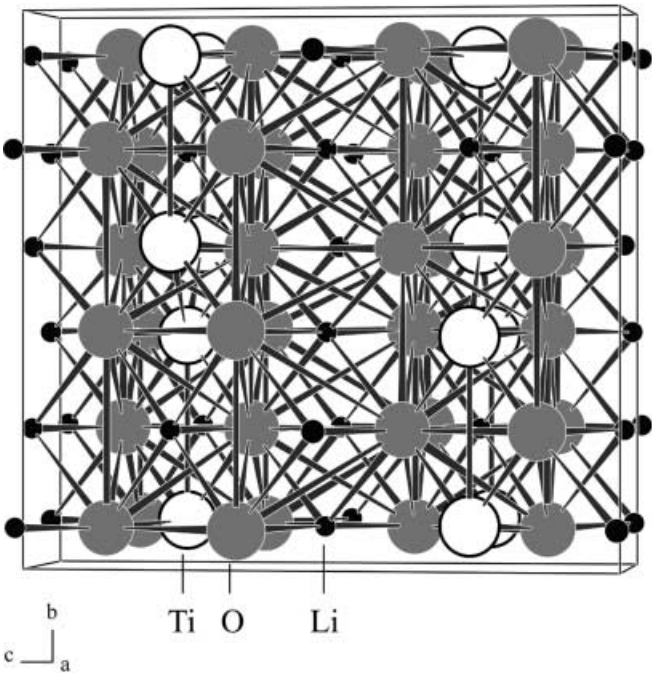

Fig. 4 Li_2TiO_3 structure: projection in *cb* plane; lithium ions are drawn in a *reduced size*

tivity. The spinel structure arrangement of atoms, partly described [25], can be used to explain possible ways for lithium ion transport. Lithium ions located on *8a* tetrahedral positions can move to empty adjacent octahedral *16c* positions and then to the next *8a* position. Each *8a* position is surrounded by four *16c* octahedra and four *16d* octahedra surrounding each *8b* site.

From the Nernst–Einstein relationship the diffusion coefficient of Li^+ at 20 °C can be estimated to be of the order 10^{-12} cm^2/s, which is comparable to another spinel-type material, $Li_xMn_2O_4$, having $D_{Li} = 10^{-9}$–10^{-8} cm^2/s [22, 23]. In $LiMn_2O_4$, lithium ion transport is released by the high electron conductivity, of the order of 10^{-4} S/cm. The significant lithium ion mobility has allowed us to use $Li_{1.33}Ti_{1.67}O_4$ as an insertion electrode material [25], as mentioned already above. Thus, this compound might be of interest for applications in electrochemical devices.

The material LT12 with the phase mixture of Li_2TiO_3 and 30.8 mol% $Li_{1.33}Ti_{1.67}O_4$, treated up to 900 °C, shows the same conductivity mechanism (E_a = 0.80(1) eV) as the pure Li_2TiO_3 below 500 °C (see Fig. 2). Below 150–200 °C the conductivity is affected by traces of sorbed water, which eliminate at 230 °C. This effect cannot be considered as a characteristic property of the material and thus is of little interest. For temperatures above 200 °C the preexponential factor is increased to $\log_e\sigma_0 = 10\times(2.2\times10^4$ S K/cm) due to a conductivity contribution from particles of $Li_{1.33}Ti_{1.67}O_4$, which however take an insufficient volume fraction (37.8 vol%) to percolate and to affect the temperature dependence of the conductivity for the pellet of LT12. The conductivity of Li_2TiO_3 is limiting. Like in pure Li_2TiO_3, a transition region is observed from 438 through 496 °C. At higher temperatures there is a short extrinsic region (496–624 °C) with an activation energy of 0.82(1) eV. It is followed by the high-temperature (> 672 °C) region of the intrinsic ion conductivity, having an activation energy of 1.08(2) eV, which is much higher than the one (0.60(2) eV) for pure Li_2TiO_3. Thus, we see that at these high temperatures the conductivity features for LT12 are remarkably different from those for the pure lithium metatitanate. It means that the structure of Li_2TiO_3 is affected by the slight amount of the solid solution of $Li_{2-4x}Ti_{1+x}O_3$ formed in the material. The presence of vacancies, introduced by Ti^{4+} substitution for lithium, provides significantly higher conductivity above 672 °C. Thus, the temperature behaviour of the conductivity confirms the existence of the solid solution in this two-phase material.

The conductivity behaviour of the two-phase materials sintered at 960 °C is more different from the properties of the pure metatitanate than the characteristics of LT12 (sintered at 900 °C). The formation of larger amounts of solid solutions has significantly changed the lithium ion transport properties in Li_2TiO_3. Three conductivity regions can be distinguished for the LT1, LT2, and LT3 specimens. At middle and low temperatures, extrinsic conductivity occurs. At middle temperatures, e.g. 300–540 °C, extrinsic-type defects caused by Ti^{4+} substitution for Li^+ determine the conductivity. Only the mobility of these charge carriers is activated and the activation energy takes values in the range 0.55–0.72 eV. Conductivity values at 300 °C vary about 10 times and are 1.5×10^{-7}, 3.5×10^{-6}, and 2.5×10^{-5} S/cm for LT1, LT2 (+13.3 mol% TiO_2), and LT3 (+25.6 mol% TiO_2), respectively. Below 300 °C the activation energy is increased (0.73–0.98 eV) as both the mobility and defect concentration are now activated. Defect (vacancy) trapping occurs on Ti^{4+} species in lithium positions. The extrinsic conductivity might be originated by ion transport in layers close to the grain surface, where the material structure is affected by the two-phase (cubic/monoclinic) interface, particularly when specimens are treated at 960 °C, where a wide range of solid solutions forms [27]. At high temperatures a more basic conductivity mechanism occurs and the mobility of all the lithium ions and vacancies determines the conductivity, having a characteristic activation energy of 1.08(3) eV for all three specimens (LT1, LT2, LT3). The conductivity values differ just a little in this region. Even higher conductivity values are expected, if the TiO_2-rich specimens could be obtained by fast cooling from temperatures above 900 °C. Then a wider range of solid solutions would be preserved. The higher concentration and mobility of the defects (vacancies) are expected to increase the conductivity in the material, as follows from Eq. 2.

Effect of high-energy irradiation on conductivity

The high-energy (5 MeV) irradiation introduces a low concentration of defects in Li_2TiO_3 [47, 48]. In Fig. 5 it is seen that irradiation remarkably increases the con-

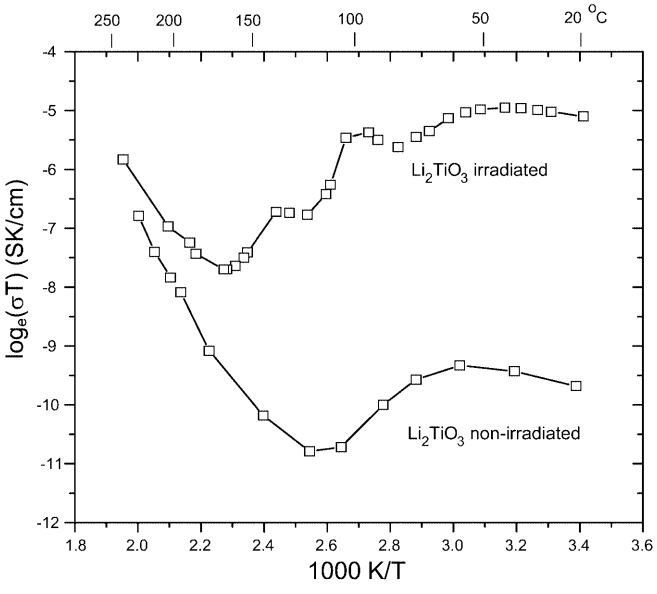

Fig. 5 Conductivity dependence on temperature for irradiated and non-irradiated Li_2TiO_3 specimens (LT14)

ductivity in Li_2TiO_3 (LT14) in the temperature range below 200 °C. Particularly, a dose of 144 MGy has increased the conductivity at 20 °C by about 100 times. However, from Fig. 5 it is also seen that sorbed water contributes to the conductivity in this temperature interval and the radiation has increased the proton conduction in the layers close to the grain surface of the ceramic samples. There must be an increase in vacancy and interstitial ion concentration when the high-energy electron excitations relax. We can expect an increase in lithium ion conductivity by a similar extent. However, the lithium ion conductivity is too low ($\sigma_{20} \approx 10^{-13}$ S/cm for non-irradiated Li_2TiO_3) to be observed. Instead, protons of the sorbed water dominate in the conductivity at temperatures below 230 °C ($\sigma_{20} = 2\times10^{-7}$ S/cm). At higher temperatures the curve of the temperature dependence of the conductivity follows values for the non-irradiated material. The sorbed water has been eliminated, and introduced defects have been annealed by this temperature.

The dependence of the conductivity on the absorbed dose is given in Fig. 6. It obeys the exponential dependence on the absorbed dose D. Parameters of the function are also given in Fig. 6. There is no saturation region obtained for the present dose interval. All the nine points, including the conductivity of the non-irradiated sample, can be fitted with a linear curve in half-logarithmic coordinates, $\log_{10}(\sigma)$ versus D. The scatter in the data points is due to the high sensitivity of the conductivity of the sorbed water to the state of the material surface.

Conclusions

The monoclinic Li_2TiO_3 is a low-conducting lithium ion conductor and lithium ions are strongly localized in their normal octahedral positions, which are occupied completely. Conductivity dependence on temperature in the coordinates $\log_e(\sigma T)$ versus $1/T$ has a transition at 500–600 °C due to a first-order phase transition and the lithium ion structure is altered, leading to the lower activation energy of the charge carrier mobility. However, these structural changes, although they were observed before, were not explained thus far. The spinel-related cubic $Li_{1.33}Ti_{1.67}O_4$ shows much higher lithium ion conductivity. Its tetrahedral lithium ions can move via adjacent octahedral positions. The temperature characteristics of the conductivity also show the effects of different mechanisms. At low temperatures, extrinsic conductivity dominates, possibly via layers close to the crystallite surface, whereas at higher temperatures (above 500 °C), intrinsic conductivity is observed. At room temperature the ion conductivity in $Li_{1.33}Ti_{1.67}O_4$ is relatively high (3×10^{-8} S/cm). Thus, this material might be of interest for applications in electrochemical devices. It has been already tested as an insertion electrode material. Of interest would be to test the effects of the introduction of vacancies by heterovalent substitution (Ti^{4+}/Nb^{5+} or Ti^{4+}/P^{5+}) in this material. This should result in higher conductivity values.

Two-phase materials ($Li_2TiO_3/Li_{1.33}Ti_{1.67}O_4$), where Li_2TiO_3 is reacted with an extra 13.3 mol% and 25.6 mol% TiO_2, show a conductivity which is determined by the Li_2TiO_3 phase as the volume fraction of 37.8 vol% for 30.8 mol% $Li_{1.33}Ti_{1.67}O_4$ is insufficient to percolate the phase mixture matrix. The ion conductivity tends to increase in these materials as lithium ions become partly substituted by Ti^{4+}. Particularly, this effect is seen for specimens sintered at 960 °C, where a wide range of solid solutions of $Li_{2-4x}Ti_{1+x}O_3$ is formed. Expressed regions of extrinsic and intrinsic conductivity are observed for these specimens as temperature characteristics of the conductivity. An increase in the conductivity, when the two-phase mixture forms, means that the diffusion of tritium charged forms and tritium release will increase as well, when the lithium burn-up occurs in the blanket zone of the fusion reactor.

The high-energy irradiation significantly increases the conductivity in Li_2TiO_3 until 230 °C. The conductivity increases exponentially from the absorbed dose. However, it is the proton conductivity caused by a slight amount of sorbed water. The conductivity is affected by the irradiation-introduced structural defects (vacancies and interstitial ions). The lithium ion conductivity is too low to be observed below 100 °C, particularly when the proton conductivity dominates. The radiation-caused increase in the proton conductivity of 100 times for a dose of 144 MGy means that a similar effect is expected for Li^+ conductivity. Lithium metatitanate is a rather durable material in high-energy radiation and thus no remarkable concentration of radiation defects can be expected after the irradiation.

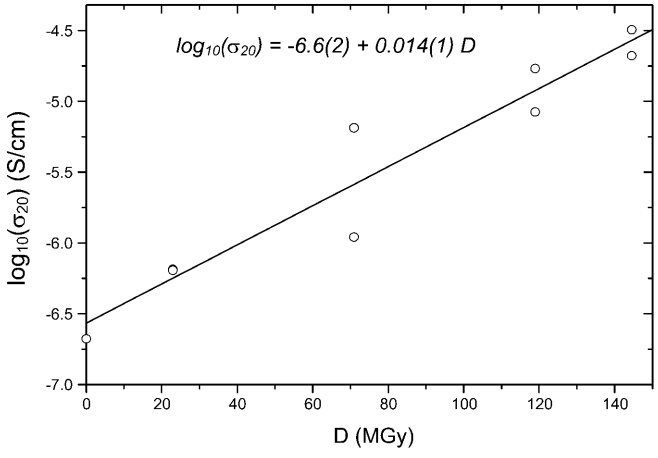

Fig. 6 Conductivity dependence on the absorbed dose D for Li_2TiO_3 (LT14) at room temperature

Acknowledgements The authors are grateful to Dr. Andris Actiņš (Chemistry Department of the University of Latvia) and to Dr. Leonīds Šebānovs (Institute of Solid State Physics of the University of Latvia) for assistance with the X-ray powder diffraction measurements.

References

1. Roux N (1997) Compilation of properties data for Li_2TiO_3. In: Noda K (ed) Proceedings of the 6th international workshop on ceramic breeder blanket interactions (JAERI conference 98-006), Mito, Japan, pp 139–147
2. Noda K, Kurasawa T, Watanabe H (1989) Adv Ceram 25:73–81
3. Konishi S, Ohno H, Hayashi T, Okuno K, Matsuo T (1990) Adv Ceram 27:173–182
4. Konishi S, Ohno H (1988) J Nucl Mater 152:9
5. Tamuzhs V, Dinduns M, Tiliks J, Vasilyev V (1991) Fusion Eng Des 17:21
6. Witingham M, Huggins R (1971) J Chem Phys 54:414
7. Wang J, Gaffari M, Choi S (1975) J Chem Phys 63:772
8. Vītiņš G, Bajārs G, Vaivars G, Kraņevskis A, Kleperis J, Lūsis A (1994) Latvian J Chem 1:78 (in Latvian)
9. Goodenough JB, Hong HY-P, Kafalas JA (1976) Mater Res Bull 11:203
10. Bayard ML, Barna GG (1978) J Electroanal Chem 91:201
11. Bukun NG, Domashnhev IA, Moskvina EI, Ukshe EA (1988) Neorg Mater 24:477 (in Russian)
12. Tuband C, Lorentz E (1914) Z Phys Chem 87:513
13. Hoshono H, Shimaji M (1974) J Phys Chem Solids 35:321
14. Ukshe EA, Bukun NG (1977) Solid electrolytes. Nauka, Moscow (in Russian)
15. Bukun NG, Mikhailova AM (1973) Elektrokhimia 9:1872 (in Russian)
16. Bykov AB, Chirkin AP, Demyanets LN, Doronin SN, Genkina EA, Ivanov-Shits AK, Kondratyuk IP, Maksimov BA, Mel'nikov OK, Muradyan LN, Simonov VI Timofeeva VA (1990) Solid State Ionics 38:31
17. Alpen UJ (1979) Solid State Chem 29:379
18. Laap T, Skaarup S, Hooper A (1983) Solid State Ionics 11:97
19. Belous AG, Novitsukaya GN, Polyanetkaya SV, Gornikov YuI (1987) Neorg Mater 23:470 (in Russian)
20. Kawai H, Kuwano J (1994) J Electrochem Soc 141:L78
21. Ohno H, Konishi S, Nagasaki T, Kurasawa T, Katsuta H, Watanabe H (1985) J Nucl Mater 132:222
22. Barker J, Pynenburg R, Koksbang R (1994) J Power Sources 52:185
23. Barker J, West K, Saidi Y, Pynenburg R, Zachau-Christansen B, Koksbang R (1995) J Power Sources 54:475
24. Massarotti V, Capsoni D, Bini M, Chiodelli G, Azzoni CB, Mozzati MC, Paleari A (1997) J Solid State Chem 131:94
25. Zachau-Christiansen B, West K, Jacobsen T, Atlung S (1990) Solid State Ionics 40–41:580
26. Mozhaev AP, Pamyatnykh AYu, Tret'yakov YuD (1980) Neorg Mater 16:2193 (in Russian)
27. Mikkelsen JC (1980) J Am Ceram Soc 63:331
28. Dubey BL, West AR (1973) J Inorg Nucl Chem 35:3713
29. Rodger AR, Kuwano J, West AR (1985) Solid State Ionics 15:185
30. Dorrian JF, Newnham RE (1969) Mater Res Bull 4:179
31. Castellanos M, West AR (1979) J Mater Sci 14:450
32. Johnston DC, Prakash H, Zachariasen WH (1973) Mater Res Bull 8:777
33. Roth RS, Parker HS, Brower WS (1973) Mater Res Bull 8:327
34. Boyce JB, Mikkelsen JC Jr (1979) Solid State Commun 31:741
35. Takahashi T, Iwahara H, Ichimura T (1970) Denki Kagaku 38:852 (in Japanese)
36. Annopol'ski VF, Belyaev EK, Tomenko VM (1971) Zh Neorg Khim 16:135 (in Russian)
37. Jung CH, Park JY, Oh SJ, Park HK, Kim YS, Kim DK, Kim JH (1998) J Nucl Mater 253:203
38. Wiles DB, Young RA (1981) J Appl Crystallogr 14:149
39. Hill RJ, Howard CJ (1987) J Appl Crystallogr 20:467
40. Madsen I, Hill RJ (1990) Powder Diffraction 5:195
41. Rietveld HM (1967) Acta Crystallogr 22:151
42. Rietveld HM (1969) J Appl Crystallogr 2:65
43. Supe A, Fedorova N, Tiliks J, Grodze J (1999) Latvian J Chem (4):52 (in Latvian)
44. Honda M (1989) A guide to measurement technology and techniques. Hewlett-Packard, Yokogawa, Japan
45. Castellanos M, West AR (1970) J Mater Sci 14:450
46. Goodenough JB (1978) Skeleton structures. In: Hagenmüller P, Van Gool W (eds) Solid electrolytes. Academic Press, New York, p 393
47. Grišmanovs V, Tanifuji T, Nakazawa T, Yamaki D, Noda K (1998) Radiation defects in Li_2TiO_3 ceramics. In: Beaumont B, Libeyre P, Gentile B, Tonon G (eds) Proceedings of the 20th symposium on fusion technology, Marseille, France, pp 1183–1186
48. Grišmanovs V, Kumada T, Tanifuji T, Nakazava T (2000) Rad Phys Chem 58:113